Motion of cells sedimenting on a solid surface in a laminar shear flow

Olivier Tissot,* Anne Pierres,* Colette Foa,* Michel Delaage,‡ and Pierre Bongrand*
*Laboratoire d'Immunologie, Hôpital de Sainte-Marguerite, 132777 Marseille Cedex 09, France; ‡Immunotech, 13288 Marseille Cedex 9, France

ABSTRACT Cell adhesion often occurs under dynamic conditions, as in flowing blood. A quantitative understanding of this process requires accurate knowledge of the topographical relationships between the cell membrane and potentially adhesive surfaces. This report describes an experimental study made on both the translational and rotational velocities of leukocytes sedimenting of a flat surface under laminar shear flow. The main conclusions are as follows: (*a*) Cells move close to the wall with constant velocity for several tens of seconds. (*b*) The numerical values of translational and rotational velocities are inconsistent with Goldman's model of a neutrally buoyant sphere in a laminar shear flow, unless a drag force corresponding to contact friction between cells and the chamber floor is added. The phenomenological friction coefficient was 7.4 millinewton · s/m. (c) Using a modified Goldman's theory, the width of the gap separating cells (6 μm radius) from the chamber floor was estimated at 1.4 μm. (*d*) It is shown that a high value of the cell-to-substrate gap may be accounted for by the presence of cell surface protrusions of a few micrometer length, in accordance with electron microscope observations performed on the same cell population. (e) In association with previously reported data (Tissot, O., C. Foa, C. Capo, H. Brailly, M. Delaage, and P. Bongrand. 1991. *Biocolloids and Biosurfaces.* In press), these results are consistent with the possibility that cell-substrate attachment be initiated by the formation of a single molecular bond, which might be considered as the rate limiting step.

INTRODUCTION

Many functions of blood leukocytes are dependent on their capacity to adhere to endothelial cells in a shear flow. Indeed, a binding event is required for migration from the blood compartment towards inflamed tissues. Several authors built flow chambers allowing continuous monitoring of the interaction between moving cells (1–3) or model particles (4) and solid surfaces. Reported data are consistent with the view that adhesion is initiated by an instant cell arrest without any requirement for a progressive velocity decrease. The adhesion efficiency is negatively correlated to the flow rate and positively correlated to the surface density of ligand molecules on interacting surfaces. However, the precise features of the initial binding event remain poorly understood. Indeed, the variations of the distance between the cell membrane and the chamber floor immediately before adhesion are not known at the nanometer level. Further, the geometrical features of the initial cell-substrate contact area are not known. This uncertainty is exemplified by the wide range of numerical estimates of initial contact areas considered in a recent model of cell adhesion (5).

An attractive way of determining the distance between flowing cells and the adherent substrate is provided by theoretical calculations performed by Goldman and colleagues (6, 7). These authors achieved accurate numerical determination of the translational and rotational velocities of a free neutrally buoyant sphere embedded in a viscous laminar shear flow near a plane wall. Their conclusions may be summarized as follows: the fluid flow exerts on the sphere a forward drag that is proportional to the shear rate (or velocity gradient). Further, when the distance δ between the sphere and the wall is much lower than the sphere radius a, the sphere is subjected to a frictional resistance to motion that is roughly proportional to its translational velocity U and $\ln(\delta/a)$. Clearly, this implies that the translational velocity U of a free sphere vanishes as $1/\ln(\delta/a)$ when δ tends to zero. Therefore, U must be a slowly varying function of δ, and the numerical value of δ may be derived from U over a wide range of concentrations. These concepts provided a suitable approach for a study of the equilibrium distance between model particles and charged surfaces (8). However, Goldman's theory has not been subjected to exhaustive experimental check. Also, the relevance of this theory to actual cells with substantial surface roughness (9) remains questionable.

In the present report, we used a flow chamber allowing continuous microscopic monitoring and digital image analysis to study both the translational and rotational motion of lymphoid cells subjected to a slow shear flow. Comparison of numerical data allowed us to

Address correspondence to: Dr. P. Bongrand, Laboratoire d'Immunologie, Hôpital de Sainte-Marguerite, BP29, 13277 Marseille Cedex 09, FRANCE.

0006-3495/92/01/204/12 $2.00

test the internal consistency of the predictions of Goldman's theory and estimate the distance between the cell surface and the chamber wall. It is concluded that actual cells cannot be considered as smooth spheres unable to interact with the surface and a specific correction to Goldman's equations is suggested. The relevance of our findings to the mechanisms of initial cell-to-substrate adhesion is discussed.

GLOSSARY

a sphere radius
d microvillus thickness
f dimensionless friction coefficient
F hydrodynamic force
G shear rate (or velocity gradient)
h distance between sphere center and plane substrate
p pressure field
R sum of sphere radius (a) and protrusion length
S microvillus area
T hydrodynamic torque
U translational velocity of the sphere
v flow velocity field
w microvillus width
α microvillus bending angle
δ distance between sphere surface and plane substrate
θ angle between vertical axis and cell protrusion
μ medium viscosity
ρ sphere density
ρ_0 medium density
Ω sphere angular velocity

THEORETICAL FRAMEWORK

We used the framework of Goldman's theory (6, 7): cells are modeled as neutrally buoyant spheres of radius a separated from a plane surface by a gap of width δ much smaller than a. Let G be the velocity gradient of the unperturbed flow, U and Ω are the translational and angular velocities of the sphere (Fig. 1).

Because G is on the order of 1 s^{-1}, a is close to 6×10^{-6} m, the medium viscosity μ is ~ 0.001 Pa · s and the medium density ρ_0 is $\sim 1{,}000$ kg/m^3, the Reynolds number $a^2 G \rho_0 / \mu$ is much smaller than unity, and the linear approximation of Navier–Stokes equation is valid:

$$\text{grad}\, p = \mu \Delta v, \tag{1}$$

where p and v are the pressure and flow velocity, respectively.

Because Eq. 1 is linear, the force F and torque T exerted on the sphere may be written as the sum of the contributions of: (a) the viscous forces due to the translation (velocity U) of a sphere parallel to the plane

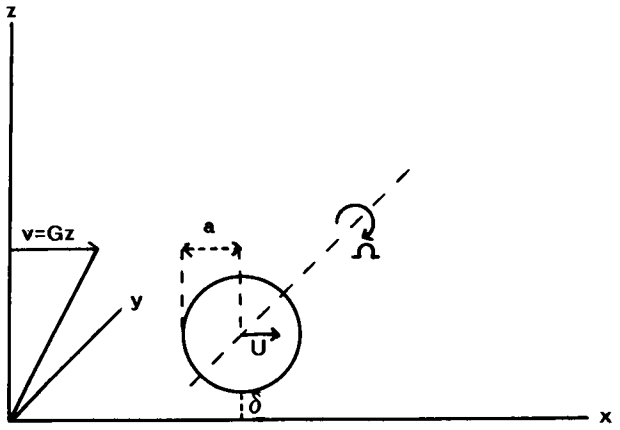

FIGURE 1 Model and coordinates. The fluid velocity V is parallel to axis Ox, and Oz is perpendicular to the chamber floor. Cells are modeled as spheres of radius a, translational velocity U, separated from the chamber floor by a gap of width δ. Ω is the angular velocity, represented by an axial vector parallel to axis Oy.

wall in absence of flow. When δ/a is small, the asymptotic lubrication theory yields (6, 7):

$$F = 6\pi\mu a U(\tfrac{8}{15} \ln(\delta/a) - 0.9588) \tag{2}$$

Translation

$$T = 8\pi\mu a^2 U(-\tfrac{1}{10} \ln(\delta/a) - 0.1895). \tag{3}$$

(b) the viscous forces due to the rotation of a sphere with angular velocity Ω in absence of flow. The lubrication theory yields (6, 7):

$$F = 6\pi\mu a^2 \Omega(-\tfrac{2}{15} \ln(\delta/a) - 0.2526) \tag{4}$$

Rotation

$$T = 8\pi\mu a^3 \Omega(\tfrac{2}{5} \ln(\delta/a) - 0.3817). \tag{5}$$

(c) The viscous drag exerted by the laminar shear flow (with velocity gradient G) on an immobile sphere close to the wall. The limiting values of the force and torque when δ is small are:

$$F = 6\pi\mu a^2 G \times 1.7005 \tag{6}$$

Shear

$$T = 4\pi\mu a^3 G \times 0.9440. \tag{7}$$

Because the total force and torque exerted on the sphere are zero when the motion is stationary, combining Eqs. 2, 4, 6 and 3, 4, 7, respectively, yields two linear equations allowing straightforward expression of U and Ω as functions of $\ln(\delta/a)$ (6, 7). Goldman's equations

read:

$$U/hG = 0.7431/[0.6376 - 0.200 \ln (\delta/a)] \quad (8)$$

$$\Omega/G = 0.4218/[0.6376 - 0.200 \ln (\delta/a)]. \quad (9)$$

As will be shown below, this theory can be easily modified by adding extra terms to Eqs. 2–7.

MATERIALS

Cells

We used DC41.1.4, a lymphoid cell clone obtained by transfecting a CD4 positive T-cell hybridoma with (*a*) α and β chain genes encoding for the T-cell receptor from an alloreactive cytotoxic T lymphocyte clone, and (*b*) a CD8α gene (10). This choice was done to allow future evaluation of the respective roles of different T-lymphocyte adhesion molecules in cell-to-substrate binding under dynamic conditions. This clone was maintained in DMEM culture medium supplemented with 10% fetal calf serum, 1 mM pyruvate, 5×10^{-5} M 2-mercaptoethanol, 0.25 mg/ml xanthine, 14 μg/ml hypoxanthine, 2 μg/ml mycophenolic acid, 2 mM L-glutamine, 100 μg/ml streptomycin and 100 u/ml penicillin. Cells were exposed to geneticin (Gibco, Glasgow, Scotland) 2 mg/ml once a month to maintain a selective pressure for transfectants.

Flow chamber

Our apparatus was described in a previous report (3). Briefly, a rectangular cavity ($17 \times 6 \times 1$ mm^3) was cut into a plexiglas block. The bottom wall of the chamber was a 22×10.5 mm^2 plastic culture coverslip (Thermanox ref. 5408; Miles Laboratory, Naperville, IL). It was stuck with silicon glue (Rubson, Brussels, Belgium) after a 15 min exposure to 5 g/l bovine albumin to prevent excessive cell attachment. Metal tubes of 1 mm internal diameter were inserted on each side of the chamber to allow cell entry and exit. The flow was generated with a plastic syringe mounted on an electric syringe holder (Razel Scientific, Stamford, CT) equipped with a 2 rpm asynchronous electric motor.

Microscopic observation

The chamber was set on the stage of an Olympus IMT2 inverted microscope (Tokyo, Japan) equipped with a Lhesa 4015 SIT videocamera (Cergy Pontoise, France) connected to a monitor through a Mitsubishi HS338 video recorder. This allowed delayed analysis of images with 13-fold slowing of cell velocity. Most studies were done with a 40× DPLANAPO 40 UV objective (Olympus; 0.85 numerical aperture). The micrometer scale used for measuring vertical displacements was carefully calibrated by sequentially focusing on the top and bottom walls of the cavity of a Neubauer hemocytometer (Elvetec, Marseille, France) (100 μm thick).

Image analysis

The main camera output was connected to a real time digitizer (PCvision+; Imaging Technology, Woburn, MA) mounted on an IBM-compatible desk computer. This provided 512×512 pixel images with 256 gray levels. A built-in digital-to-analogue converter allowed continuous display of digitized images. An assembly language program was written in the laboratory to control processing (11). The following procedure was used to monitor cell motion with maximum accuracy: a mouse-controlled cursor was programmed to allow the observer to follow moving cells on a monitor screen. Small (64×24 pixel size) pieces of the whole image were transferred to the host computer memory at regular intervals. These images were subjected to delayed analysis for determination of cell position and localization of surface asperities. Under standard conditions, the pixel width was 0.43 μm.

Electron microscopy

Cells were fixed with glutaraldehyde (1%) in pH 7.2 cacodylate buffer (0.05 M) supplemented with 0.05% ruthenium red to stain the glycocalyx (12). After 60 min at 4°C, cells were rinsed for 2 h in cacodylate buffer (0.07 M) and postfixed for 3 h in 1% osmic acid solution containing 0.1% ruthenium red and 0.1 M cacodylate buffer. Cells were then dehydrated and embedded in epon for examination in a Jeol 200C electron microscope.

RESULTS

Cells roll for long periods of time with fairly constant velocity

First, the flow conditions were carefully calibrated by studying suspensions of small diameter latex beads and focusing at different distances from the chamber floor. As shown on Fig. 2, the velocity gradient G was fairly constant in a region much thicker than the cell diameter. The same flow conditions ($G = 1.32$ s^{-1}) were used throughout all experiments.

Individual cells were observed. The focus was chosen in order to make rolling cells appear as bright disks with dark boundaries. As shown in Fig. 3, repeated digitization of sequential frames allowed accurate monitoring of cell location. A typical trajectory is depicted in Fig. 4. Obviously, the cell abscissa was a fairly linear function of time for periods of several seconds, thus ensuring that the sedimentation process was essentially terminated. However, significant fluctuations of the cell position with respect to the mean straight line were clearly visible (Fig. 4).

Cell velocity is not strongly correlated to cell size or shape

Twenty different cells were assayed for translational velocity U and radius a. The mean value of the dimensionless parameter U/aG was 0.91 (0.045 SE of the mean, range 0.75–1.80). There was no significant correlation between parameters a and U (Fig. 5; the correlation coefficient is 0.30).

Because cells often displayed irregular shapes (which was indeed a useful feature, as shown below), it was important to know whether U/aG was correlated to the cell ellipticity (i.e., the ratio b/a between the smallest and largest axis lengths, a and b). This possibility was

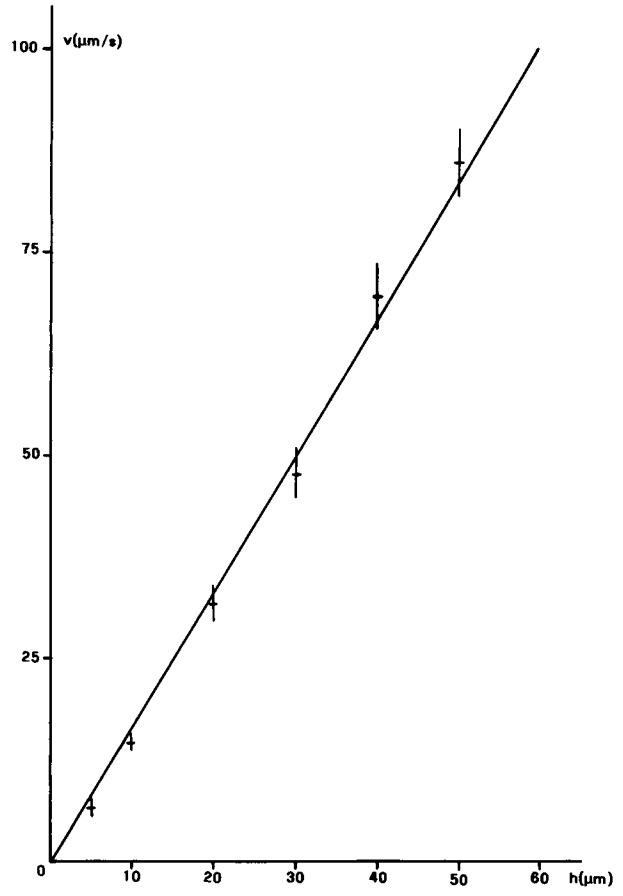

FIGURE 2 Calibration of the hydrodynamic flow. A suspension of 0.8 μm diameter latex beads was driven through the flow chamber and the translational velocity was measured at different distances from the chamber floor. Each point represents a mean of at least 20 separate measurements. Vertical bar length is twice the standard error of the mean.

tested on a sample of 11 cells with ellipticity ranging between 1.04 and 1.51 (mean: 1.19). As shown on Fig. 6, no substantial correlation was found between both parameters. However, it was noticed that the largest cell axis remained perpendicular to the translational velocity.

Goldman's theory cannot account for cell movement

In view of the above data, it appeared reasonable to model cells as spheres. It was thus tempting to use Goldman's equations (7) to derive the distance between moving cells and the chamber floor from the numerical value of parameter U/aG. However, it seemed of interest to check the relevance of the theory to actual rolling cells. This was done by selecting cells with prominent surface patterns (Fig. 3) and measuring both translational and rotational velocities. Results are shown in Table 1. These figures are clearly inconsistent with Goldman's theory. Indeed, the theoretical value of $U/\Omega a$ ranged between infinity (large cell-to-wall distance) and 1.76 (close contact). However, the mean experimental value of this parameter was 1.45, and 10 individual values out of 11 were <1.76 (not shown).

Further, the experimental value of U/aG (i.e., 0.86) was suggestive of a width of 0.77 μm for the distance between cells and the chamber floor (for a sphere of 6 μm radius). The expected value of $U/a\Omega$ would thus be 2.22, in contrast with the experimental value.

Experimental data are consistent with a model including a friction between cells and the chamber wall

The simplest phenomenon likely to account for the high cell angular velocity was a friction force between the cell surface and the chamber floor. In order to test this possibility, we modified Goldman's equations by adding a phenomenological friction coefficient f corresponding to a rearward drag proportional to the cell surface velocity near the wall (this was equal to $U - \Omega a$). The resulting force F and torque T are:

$$F = -6\pi\mu a f (U - \Omega a) \tag{10}$$

Friction

$$T = 6\pi\mu a^2 f (U - \Omega a). \tag{11}$$

Eqs. 10 and 11 were combined with Eqs. 2–7. Writing that the total force and torque exerted on the sphere were zero, we obtained modified Goldman's equations. After proper simplification, the equilibrium equations read:

$$(\tfrac{8}{15}\ln(a/\delta) + 0.9588 + f)(U/aG) + (0.2526 - \tfrac{2}{15}\ln(a/\delta) - f)(\Omega/G) = 1.7005 \tag{12}$$

$$(0.3790 - \tfrac{1}{5}\ln(a/\delta) - 1.5f)(U/aG) + (0.7634 + \tfrac{4}{5}\ln(a/\delta) + 1.5f)(\Omega/G) = 0.9440. \tag{13}$$

These equations were solved numerically, using different values for parameter f. Results are displayed on Fig. 7. Thus, experimental data (Fig. 7, *solid circle*) are consistent with the framework of Goldman's theory provided a drag force F is added to other hydrodynamic interactions:

$$F = f(U - \Omega a); \quad f/6\pi\mu a = 0.65 \tag{14}$$

$$f = 7.35 \times 10^{-8}\ \mathrm{N \cdot s/\mu m}, \tag{15}$$

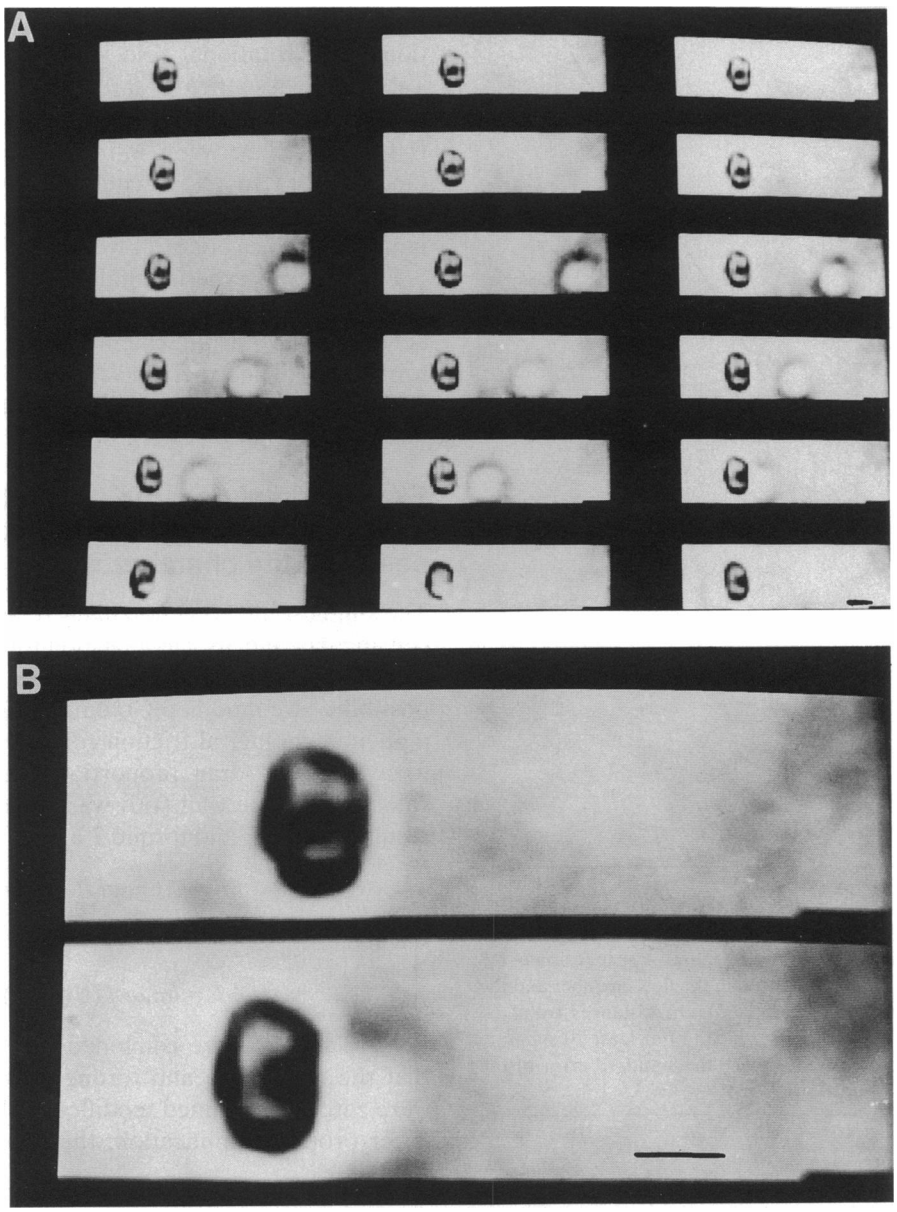

FIGURE 3 Microscopical observation of flowing cells. Lymphoid cells (41.1.4 line) were subjected to a laminar shear flow under continuous microscopic observation. (*A*) 18 digitized images of a single cell are shown (the total period of time is ~1 s). (*B*) The first and 15th frames are displayed on the same monitor. They are separated by a period of 0.77 s and the cell anterior edge moved by 5.2 μm. The dark area visible on the cell surface represents a protrusion whose displacement relative to the cell edge was monitored in order to appreciate the angular velocity of the moving cell. Bar length is 12.5 μm.

where μ is the medium viscosity. It was found suitable to use a dimensionless friction parameter.

The width of the dimensionless cell-substrate gap was:

$$\delta/a = 0.24, \qquad (16)$$

corresponding to a gap of ~1.4 μm for a cell of 6 μm radius.

Cell surface protrusions may account for the high value of the cell-substrate gap

Clearly, repulsive electrostatic forces or steric stabilization cannot account for the estimated value of parameter δ (13, 14). Hence, a reasonable hypothesis would be

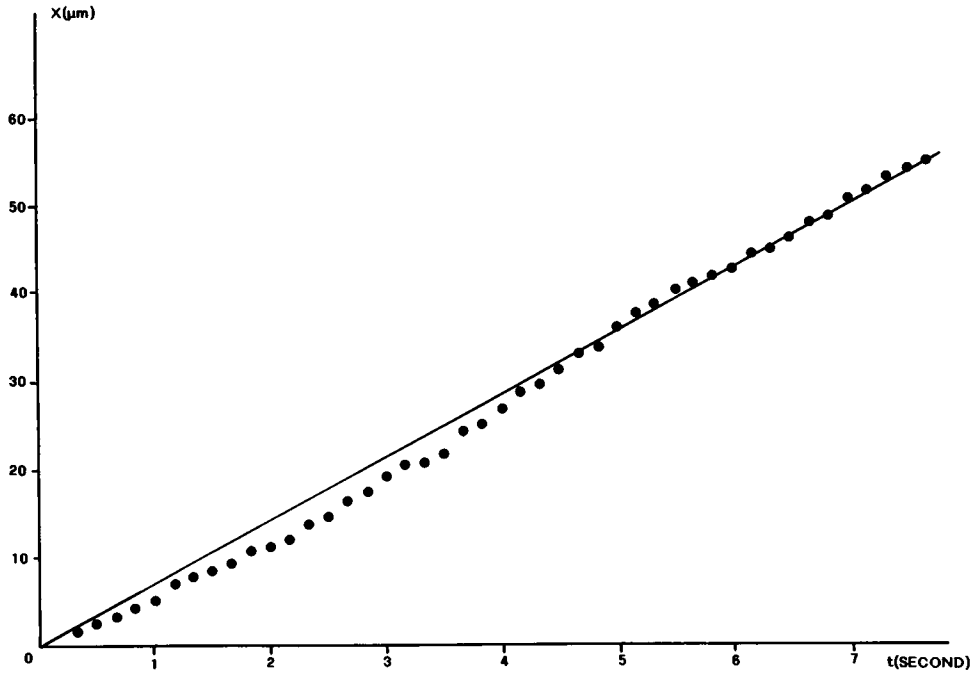

FIGURE 4 Translational motion of a rolling cell. The position of the anterior edge of a single rolling cell was determined at regular intervals of ~0.17 s, allowing accurate study of short term velocity variations. Mean velocity is 7.1 μm/s.

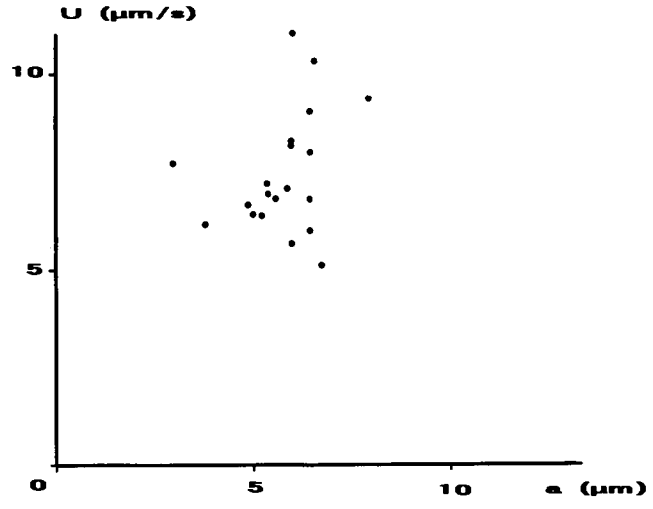

FIGURE 5 Lack of correlation between cell radius and translational velocity in a laminar shear flow. 20 individual cells were studied for determination of translational velocity U and radius a. These parameters were not significantly correlated ($P > 0.05, r = 0.30$).

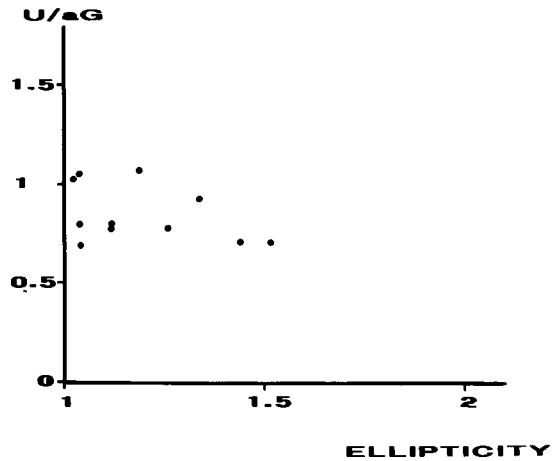

FIGURE 6 Lack of correlation between cell ellipticity and translational velocity. 11 individual cells subjected to a laminar shear in the chamber flow were monitored for determination of translational velocity U and the size of the largest (b) and smallest (a) axis length. The dimensionless parameter U/aG was plotted versus ellipticity b/a. There was no significant correlation between both parameters ($r = 0.36$, $P > 0.05$).

TABLE 1 **Translational and rotational velocity of flowing cells**

	Translational velocity U	Rotational velocity Ω	U/aG	Ω/G	$U/\Omega a$
	μm/s	*rad/s*			
Mean	7.07	0.78	0.86	0.59	1.45
Standard error	0.36	0.064	0.043	0.048	0.098

Cell suspensions were driven through a flow chamber with a wall shear rate G of 1.32 s^{-1}. Clearcut surface asperites were selected and their translational and rotational velocities were determined by analyzing series of digitized frames. Eleven individual cells were studied. Mean values are shown together with standard errors (mean). Mean cell radius was 6.3 μm (standard error 0.086).

that cell surface microvilli generated upward forces on rolling cells when these encountered the channel surface. Indeed, electron microscopy showed that the cells we studied were studded with numerous surface protrusions (Fig. 8).

This possibility was subjected to quantitative analysis by considering the movement of a sphere with a thin rigid protrusion and incorporating into Goldman's equations, in addition to the aforementioned friction force, a sedimentation force (i.e., cell weight minus buoyancy), a vertical hydrodynamic force generated by the relative

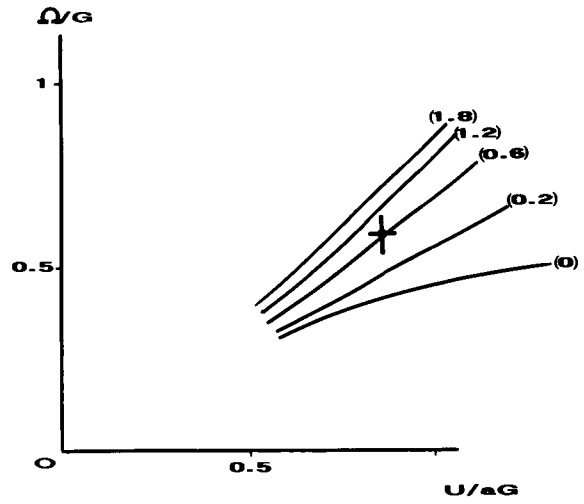

FIGURE 7 Effect of surface friction on the movement of a sphere near a plane wall in a laminar shear flow. Goldman's theory (based on lubrication theory) was used to determine the angular velocity (Ω) and translational velocity (U) as a sphere of radius a at varying distance δ from the wall. G is the shear rate (or velocity gradient). The friction force was expressed with a phenomenological parameter f and different plots or Ω/G versus U/aG were constructed for various values of the dimensionless parameter $f/6\pi\mu a$ (values are shown in brackets; μ is the medium viscosity). The solid circle represents the experimental data averaged on 11 separate cells. Vertical and horizontal bar length represent twice the standard error of the mean.

displacement of the cell and the wall, and the contact force obtained by considering the equilibrium of vertical forces. This contact force was considered as vertical because the friction component was included in parameter f. Cells were thus modeled as spheres of radius a with a rodlike protrusion OP of length R (see Fig. 9 A for the definition of coordinates. Note that the algebraic convention for angles is unusual, in order that θ be positive when the rotational velocity is positive with respect to axis Oy). Now, we shall add two interactions to the viscous forces included in Goldman's theory supplemented with a friction term.

(a) A hydrodynamic force is generated by the mutual displacement of a cell and the wall (15–17). We made use of a formula first derived by Taylor and applied by Dimitrov to cells. This may be approximated by the following interpolation formula (18):

$$F_v = -(6\pi\mu a^2/\delta)d\delta/dt. \quad (17)$$

(b) Cells are subjected to a sedimentation force of gravitational origin:

$$F_p = -(4/3)\pi a^3(\rho - \rho_0)g, \quad (18)$$

where ρ and ρ_0 are the cell and medium volumic mass, and g is the gravity acceleration. The hydrodynamic interaction between the protrusion tip and the wall is expected to be negligible as long as molecular contact is not achieved, due to the very slow (logarithmic) increase of this interaction when the separating gap decreases. The vertical component F_R of the wall reaction may be obtained by considering equilibrium equations along the vertical axis Oz. We obtain:

$$F_R = 6\pi\mu a^2 R \sin\theta/(R\cos\theta - a) \times d\theta/dt - 4\pi a^3(\rho - \rho_0)g/3. \quad (19)$$

The horizontal component is accounted for by the phenomenological friction parameter f.

Now, the movement of a villous cell may be viewed as follows: (a) when a protrusion of length R encounters the chamber floor, it experiences a vertical force F_R resulting in additional torque:

$$T_R = F_R R \sin\theta, \quad (20)$$

this must be incorporated into Goldman's equations, using the geometrical relationship:

$$\delta = R\cos\theta - a, \quad (21)$$

which yields:

$$[(8/15)\ln(a/\delta)20.95888 + f]U/aG + [0.2526 - (2/15)\ln(a/\delta) - f]\Omega/G = 1.7005 \quad (22)$$

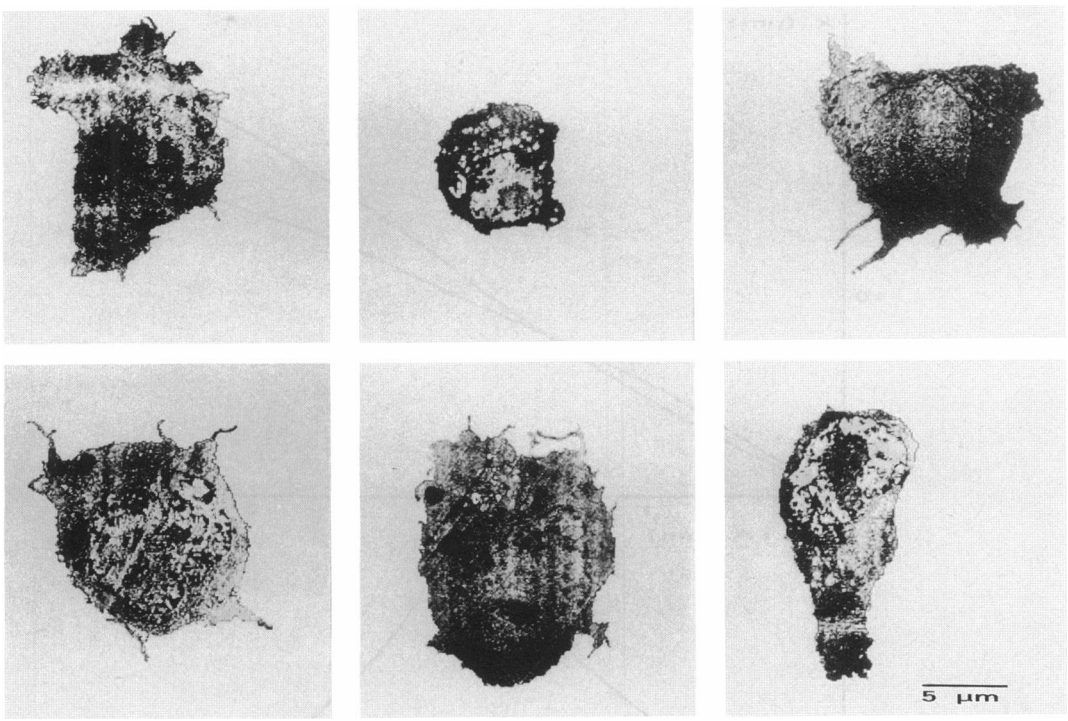

FIGURE 8 Electron microscopical study of flowing cells. Cells from the 41.1.4 line were studied with electron microscopy. Several typical images are shown, thus demonstrating the occurrence of surface protrusions of several micrometer length. Bar length is 5 μm.

$$[0.3790 - (1/5)\ln(a/\delta) - 1.5f]U/aG + [0.7634 + (4/5)\ln(a/\delta) + 1.5f + \ldots \ldots 1.5(R/a)^2 \sin^2\theta]\Omega/G = 0.9440 + (\rho - \rho_0)gR\sin\theta/3\mu G, \quad (23)$$

(*b*) when θ becomes positive (Fig. 9 *C*), the motion equations depend on the sign of the righthand term of the above equation for F_R. If this is negative, the above equations remain valid. Otherwise, the cell protrusion separates from the wall (Fig. 9 *E*). The variations of the gap width δ are obtained by considering the balance between sedimentation force and hydrodynamic repulsion. We obtain:

$$d\delta/dt = (2/9)(\rho - \rho_0)ga\delta/\mu. \quad (24)$$

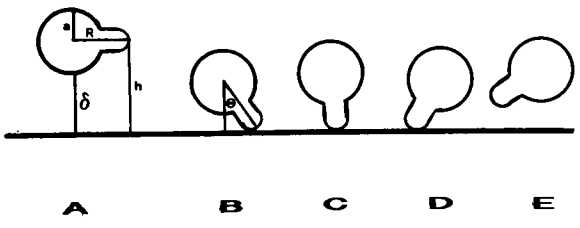

FIGURE 9 Movement of a cell with a rigid protrusion. (*A*) Free rotation at a distance from the wall. (*B*) Due to sedimentation and rotation, the protrusion encounters the wall, generating a repulsive force. (*C*) Neutral position. (*D*) Sedimentation and contact reaction increase the cell angular velocity. (*E*) The protrusion separates from the chamber wall, whereas the cell-to-substrate gap goes on decreasing.

The above equations were used to derive numerically the motion of rolling cells, using steps of 0.02 s. Representative curves are shown on Fig. 10 and additional numerical data are displayed on Tables 2 and 3. The main conclusions are as follows: (*a*) the distance between the cell and the wall may display substantial oscillatory behavior, with concomitant variation of translational velocity. Thus, when the distance between a cell (6 μm diameter) and the substrate varied between 0.5 and 1.5 μm due to the presence of a protrusion of 1.8 μm length, the translational velocity was increased by 36%. (*b*) When the numerical values of the protrusion length (Table 2) and friction force (Table 3) were varied, it appeared that friction dramatically increased cell angular velocity (Table 3). The major effect of cell protrusions was to increase the distance between the cell and chamber wall. (*c*) The experimental features of cell motion are consistent with the view that cells may be modeled as spheres studded with rigid protrusions of a

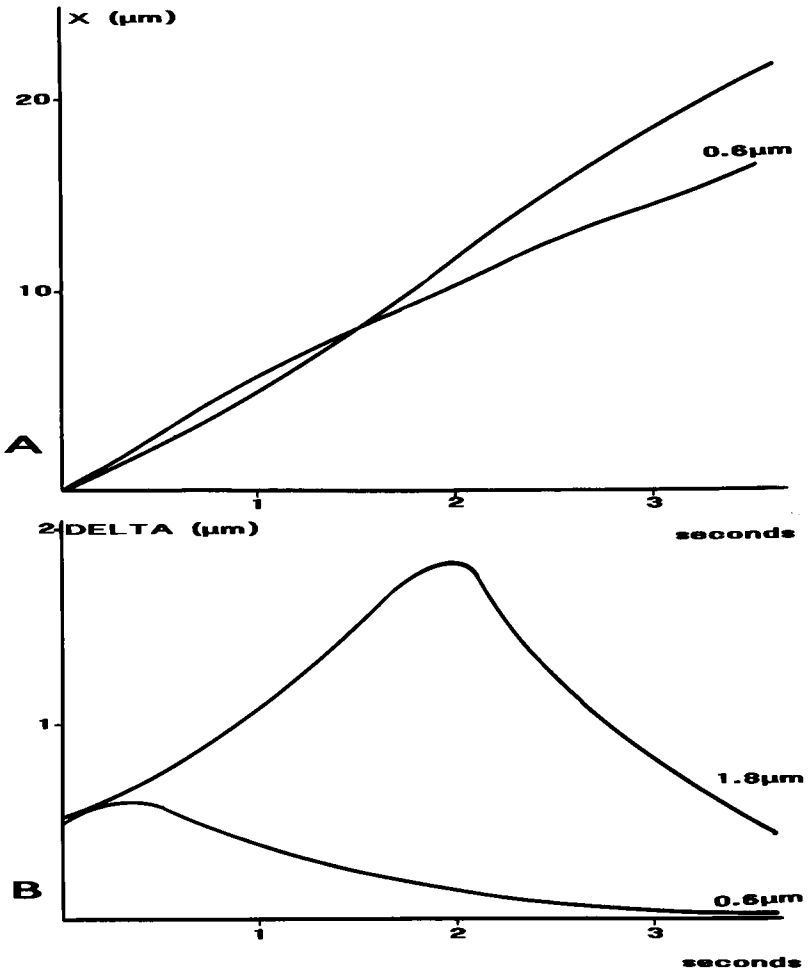

FIGURE 10 Movement of a cell with a rigid protrusion: numerical simulation. The movement of a cell of 6 μm radius with a protrusion of 1.8 μm (*solid lines*) or 0.6 μm (broken lines) was simulated using 0.65 for the dimensionless friction coefficient. Initial conditions are as shown on Fig. 7 *B*, with a 0.5 μm gap between the cell and the substrate floor. The cell abscissa (8 *A*) and cell-to-substrate gap δ (8 *B*) are shown for a period of 3 s.

TABLE 2 Influence of protrusion length on cell motion near a plane wall

Protrusion length	Abscissa x	$\langle U/aG \rangle$	$\langle \Omega/G \rangle$	δ_f	δ_f/a
μm	μm			μm	
1.8	18.3	0.77	0.04	0.75	0.125
1.2	17.1	0.72	0.41	0.25	0.042
0.6	14.5	0.61	0.39	0.054	0.009

The motion of a rolling cell with a protrusion of variable length was determined for a period of 3 s by numerical solution of the equations of motion (using steps of 0.02 s). Initial conditions were (*a*) 0.5 μm gap between cell and surface and (*b*) contact between the protrusion and the surface (Fig. 7 *A*). U and Ω are the translational and rotational velocities. The velocity gradient G is 1.32 s^{-1}, the cell radius a is 6 μm. Brackets ($\langle\ \rangle$) are for mean values, δ_f is the width of the cell-to-substrate gap at the end of the 3 s interval.

TABLE 3 Influence of the friction coefficient on cell motion near a plane wall

Dimensionless friction coefficient	$\langle U/aG \rangle$	$\langle \Omega/G \rangle$
$(f/6\pi\mu a)$		
0	0.82	0.04
0.5	0.79	0.32
1	0.74	0.41
2	0.68	0.48

The motion of a rolling cell of 6 μm radius (parameter a) with a rigid protrusion of 1.8 μm length was determined for a period of 3 s by numerical solutions of the equations of motion. Initial conditions are as described in Table 2 (0.5 μm gap, initial contact between chamber floor and cell protrusion). The velocity gradient G is 1.32 s^{-1}. U and Ω are the translational and rotational velocities, respectively, brackets ($\langle\ \rangle$) denote mean values.

few micrometer length, and translational movement is impeded by short range interactions with cells and the chamber floor.

DISCUSSION

The present work was designed to yield precise information on the topographical relationships between a fixed substrate and mobile cells subjected to a laminar shear flow. This is indeed a prerequisite to a thorough understanding of the initial step of cell-to-substrate attachment such as occurs in flowing blood. The basic idea was to use irregular shaped cells, thus allowing monitoring of both translation and rotation of moving elements. Also, a fairly low shear rate was chosen in order to permit accurate monitoring of the motion with a standard videocamera.

The first conclusion was that cells moved for prolonged periods of time with fairly constant velocity, in accordance with previous reports (1, 2, 3). Although cells occasionally adhered to the substrate after an immediate arrest, the motion was not altered when the chamber room was coated with adhesive molecules (reference 3 and data not shown). It is therefore suggested that cell translation did not involve substantial formation and breakage of intermolecular bonds with the plane surface.

A second unambiguous conclusion was that the translational velocity of flowing cells was not substantially slower than the unperturbed fluid velocity near the cell center of gravity. Using the framework of Goldman's theory, it is thus strongly suggested that the major part of the cell membrane was not in molecular contact with the surface of the flow chamber. Indeed, a value of 0.86 for the dimensionless velocity U/aG would lead to a distance of ~ 0.8 μm between the substrate and cells modeled as spheres of 6 μm radius.

Thirdly, simultaneous measurement of the translational and rotational velocities of individual cells yielded experimental values that were clearly inconsistent with Goldman's theory. Additional data suggested that this discrepancy was not due to the ellipticity of actual cells (Fig. 6). Hence, the simplest hypothesis was that local friction forces were generated by cell-to-substrate interaction. It was indeed shown that experimental data were fully compatible with a modified Goldman's theory including a phenomenological friction term (Fig. 7). Considering cells of 6 μm radius, the width of the cell-substrate gap would be ~ 1.4 μm, and the ratio between the drag force and the relative cell-substrate velocity would be ~ 74 nanonewton · s/μm in a medium of 0.001 Pa · s viscosity.

Fourthly, it was checked that the high suggested value of the cell-to-substrate gap was physically admissible. Indeed, the balance between gravity and cell-to-substrate repulsion is expected to result in an equilibrium distance much lower than 1.4 μm (13, 14). Also, hydrodynamic lifting forces possibly generated by the cell translation are expected to be negligible due to the low value of the shear rate used in our study (15, 16). It was thus hypothesized that cell surface protrusions might exert an upward push on the cells. Hydrodynamic cell-to-substrate interaction might substantially decrease ensuing sedimentation rate (17, 18). This process was incorporated in Goldman's theory. As shown in Fig. 10, a single protrusion of 1.8 μm length might raise cell-to-substrate distance above 1 μm for ~ 1.8 s, corresponding to about a fourth of a turn (using the experimental value of 0.78 for cell angular velocity). Hence, a few cell surface microvilli or lamellipodia might suffice to maintain a relatively high cell-to-substrate distance. This is clearly consistent with electron microscopic data. Note that the influence of cell surface asperities on mutual approach in a shear flow was well discussed by Goldsmith and colleagues (19). However, three particular points deserve some comments.

(*a*) Our model requires that cell surface lamellipodia behave as rigid structures during their interaction with the substrate. Although precise data on the mechanical behavior of cell surface microvilli are lacking, it may be argued that the mere viscosity of submembranar cytoplasm might prevent rapid bending of a lamellipodium. Indeed, consider a sheet of thickness h and width w protruding above the cell membrane by length L. Assume that this veil bends with constant thickness, thus acquiring the shape of a circular line subtended by angle α (Fig. 11). The mutual displacement between faces is on the order of αh, resulting in tangential stress $F \approx \mu\alpha/t$, where t is the duration of the bending process and μ the cytoplasmic viscosity. The work dissipated during this process is obtained by multiplying the lifting push P with the displacement of the tip of the lamellipodium, which is on the order of αh. Hence, we obtain:

$$Pw\alpha \approx (\mu\alpha/t) \times (wL) \times (\alpha h). \tag{25}$$

Hence:

$$P \approx \mu\alpha Lh/t. \tag{26}$$

Taking 100 Pa · s for the cytoplasm viscosity (20), we conclude that the force required to bend a lamellipodium of length 1 μm by an angle of 1 radian is $\sim 10^{-11}$ newton. This is more than 10 times the sedimenting force. Clearly, cytoplasmic viscosity might well allow cell

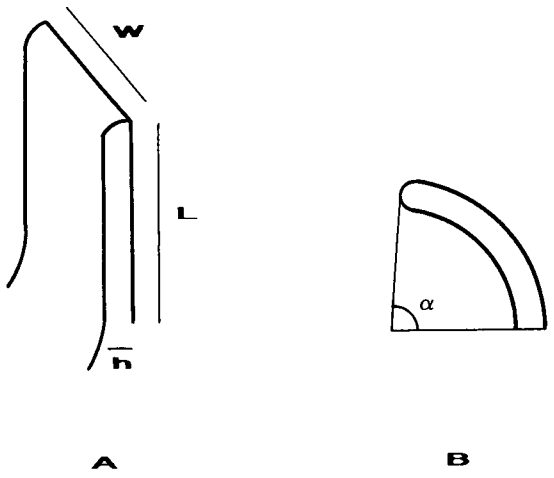

FIGURE 11 Limitation of lamellipodium bending by viscous forces. A lamellipodium is modeled as a sheet of thickness h, width w, and length L. Bending requires parallel sliding of limiting faces, with concomitant generation of viscous forces.

surface lamellipodia to resist bending and push cells at distance from the substrate.

(*b*) In a previous study made on rat thymocytes (3), it was found that smoothing cell surfaces by exposure to hypotonic media did not substantially alter translation velocity. However, cell rotational velocity could not be measured in the same study. It may be argued that the departure from a spherical shape may suffice to maintain fairly high cell-to-substrate distance, cells behaving as "imperfect wheels" subjected to repeated upwards pushes during their displacement. Further, because the derivation of cell-substrate distance from velocity determinations is not very accurate, due to the logarithmic dependence of velocity on distance, it is difficult to compare the translation velocities of two cell samples subjected to similar hydrodynamic flow.

(*c*) The influence of cell vertical displacement on translational motion (Fig. 9 *A*) is in qualitative agreement with experimental data.

A final point is about the experimental value of the friction coefficient we obtained. If the region of closest interaction between the cell and the chamber floor is modeled as a gap of width d separating parallel plates, the drag coefficient is expected to be on the order of $\mu S/d$, where μ is the medium viscosity and S is the area of the tip of a microvillus or lamellipodium. Using 0.01 μm^2 and 0.01 μm as reasonable orders of magnitude for S and d, the experimental value of 74 $nN \cdot s/\mu m$ suggests that the effective viscosity of the medium in the cell-substrate gap is higher than the bulk medium viscosity by two orders of magnitude. The most likely explanation for this finding would be that the flow is hampered by glycocalyx molecules bound to the cell surfaces and behaving as a porous network (21).

The overall conclusion of this study is therefore that rolling cells are in contact with the substrate over very limited areas (corresponding to the tip of microvilli). A single bond might be responsible for initial cell arrest. Indeed, the energy of such a bond may well tether a cell against the fluid flow (22, 23) until adhesion is strengthened by cell deformations (9) and lateral concentration of adhesion molecules (24).

It is planned to subject these concepts to direct experimental test by studying the adhesion of cells to substrates coated with controlled amounts of adhesion molecules, using fluorescent labeling and confocal scanning laser microscopy.

This work was supported by a grant from the INSERM (CJF 89.07).

Received for publication 6 May 1991 and in final form 19 August 1991.

REFERENCES

1. Doroszewski, J., J. Skierski, and L. Przadka. 1977. Interaction of neoplastic cells with glass surface under flow conditions. *Exp. Cell Res.* 104:335–343.
2. Forrester, J. V., and J. M. Lackie. 1984. Adhesion of neutrophil leukocytes under conditions of flow. *J. Cell Sci.* 70:93–110.
3. Tissot, O., C. Foa, C. Capo, H. Brailly, M. Delaage, and P. Bongrand. 1991. Influence of adhesive bonds and surface rugosity on the interaction between rat thymocytes and flat surfaces under laminar shear flow. *Biocolloids and Biosurfaces.* In press.
4. Wattenbarger, M. R., D. J. Graves, and D. A. Lauffenburger. 1990. Specific adhesion of glycophorin liposomes to a lectin surface in shear flow. *Biophys. J.* 57:765–777.
5. Hammer, D. A., and D. A. Lauffenburger. 1987. A dynamical model for receptor-mediated cell adhesion to surfaces. *Biophys. J.* 52:475–487.
6. Goldman, A. J., R. G. Cox, and H. Brenner. 1967. Slow viscous motion of a sphere parallel to a plane wall. I. Motion through a quiescent fluid. *Chem. Eng. Sci.* 22:637–651.
7. Goldman, A. J., R. G. Cox, and H. Brenner. 1967. Slow viscous motion of a sphere parallel to a plane wall. II. Couette flow. *Chem. Eng. Sci.* 22:653–660.
8. Prieve, D. C., and B. M. Alexander. 1986. Hydrodynamic measurement of double-layer repulsion between colloidal particle and flat plate. *Science (Wash. DC).* 231:1268–1270.
9. Mège, J. L., C. Capo, A. M. Benoliel, and P. Bongrand. 1987. Use of cell contour analysis to evaluate the affinity between macrophages and glutaraldehyde-treated erythrocytes. *Biophys. J.* 52:177–186.
10. Letourneur, F., J. Gabert, P. Cosson, D. Blanc, J. Davoust, and B. Malissen. 1990. A signaling role for the CD8α cytoplasmic segment revealed under limiting stimulatory conditions. *Proc. Natl. Acad. Sci. USA.* 87:2339–2343.

11. André, P., A. M. Benoliel, C. Capo, C. Foa, M. Buferne, C. Boyer, A. M. Schmitt-Verhulst, and P. Bongrand. 1990. Use of conjugates made between a cytolytic T cell clone and target cells to study the redistribution of membrane molecules in cell contact areas. *J. Cell Sci.* 97:335–347.
12. Cook, G. M. W., and R. W. Stoddart. 1973. Surface carbohydrates of the eukaryotic cell. Academic Press Limited (AP), London. 56–97.
13. Bongrand, P., and G. I. Bell. 1984. Cell-cell adhesion: parameters and possible mechanisms. *In* Cell Surface Dynamics—Concepts and Models. A. S. Perelson, C. DeLisi, and F. W. Wiegel, editors. Marcel Dekker Inc., New York. 459–493.
14. Bongrand, P., Editor. 1988. Physical Basis of Cell-Cell Adhesion. CRC Press. Boca Raton, FL. 267 pp.
15. Saffman, P. G. 1965. The lift on a small sphere in a slow shear flow. *J. Fluid Mech.* 22:385–400.
16. Blackshear, P. L., R. J. Forstrom, F. D. Dorman, and G. O. Voss. 1971. Effect of flow on cells near walls. *Fed. Proc.* 30:1600–1609.
17. Brenner, H. 1961. The slow motion of a sphere through a viscous fluid towards a plane surface. *Chem. Eng. Sci.* 16:242–251.
18. Dimitrov, D. S., N. Stoicheva, and D. Stefanova. 1984. A simple interpolation formula for the rate of approach of particles or cells with tension-controlled shapes at arbitrary separation. *J. Colloid Interface Sci.* 98:269–271.
19. Goldsmith, H. L., O. Lichtarge, M. Tessier-Lavigne, and S. Spain. 1981. Some model experiments in hemodynamics: VI. Two-body collisions between blood cells. *Biorheology.* 18:531–555.
20. Evans, E., and A. Yeung. 1989. Apparent viscosity and cortical tension of blood granulocytes determined by micropipet aspiration. *Biophys. J.* 56:151–160.
21. Wiegel, F. W. 1980. Fluid flow through porous macromolecular systems. Springer-Verlag, Berlin, 102 pp.
22. Bell, G. I. 1988. Models of cell adhesion involving specific bonds. *In* Physical Basis of Cell–Cell Adhesion. P. Bongrand, editor. CRC Press. Boca Raton, FL. 227–258.
23. Evans, E., D. Berk, and A. Leung. 1991. Detachment of agglutinin-bonded red blood cells. I. Forces to rupture molecular point attachments. *Biophys. J.* 59:838–848.
24. Bell, G. I., M. Dembo, and P. Bongrand. 1984. Cell adhesion. Competition between nonspecific repulsion and specific bonding. *Biophys. J.* 45:1051–1064.